ELSEVIER

Journal of Power Sources 74 (1998) 34–39

JOURNAL OF POWER SOURCES

Effects of surface treatment on performances of metal hydride electrodes and Ni/MH batteries

Weixiang Chen [a,*], Zhiyuan Tang [b], Hetong Guo [b], Zhaolin Liu [b], Changpin Chen [a], Qidong Wang [a]

[a] *Dept. of Materials Science and Engineering, Zhejiang University, Hangzhou 310027, China*
[b] *Dept. of Applied Chemistry, Tianjin University, Tianjin 300072, China*

Received 18 August 1997; accepted 18 December 1997

Abstract

Metal hydride (MH) electrodes are treated in an alkaline solution containing potassium borohydride (KBH_4) to increase the discharge capacity and high-rate dischargeability and to improve the activation, electrocatalytic activity and cyclic stability. XPS and ICP analyses indicate that the nickel oxide on the surface of the hydrogen-storage alloy is partly reduced by the reduction treatment. Part of the atomic hydrogen released during this treatment is adsorbed on the surface of the alloy and penetrates into the lattice to form the hydride. It is found that a Ni-rich surface layer with a high electrocatalytic activity for the electrode reaction is produced because of the preferential dissolution of Mn and Al. In addition, the specific surface area of the treated alloy is increased. An AA-size Ni–MH battery has been assembled with the treated MH electrode as its negative electrode. The battery displays a superior high-rate dischargeability and better low-temperature characteristics.

Keywords: Metal hydride electrode; Potassium borohydride; Surface treatment; Ni–MH battery

1. Introduction

Nickel–metal hydride (Ni–MH) rechargeable batteries have attracted increasing attention because of several inherent advantages, namely, high specific energy and power, high-rate charge–discharge capability, high tolerance to overcharge–overdischarge, environmental acceptance (avoidance of Cd) [1]. So far, many multi-component, mischmetal-based, hydrogen-storage alloys have been developed to meet the requirement of high cycling life [1–4]; these include substitution of the nickel by Mn, Co and Al. The composition of the alloy is important, and the effects of surface composition and morphology are also significant. Micro-encapsulation of the alloy powder particles with an electroless coating of copper or nickel alloy has been confirmed [5,6] to be effective in improving the performance of hydride negative electrodes.

In this paper, a study is made of the effects of a surface reduction treatment (performed in an alkaline solution with reducing agent) on the performance of MH electrodes. The characteristics of an AA-size battery with the treated MH electrode as the negative electrode are also reported.

2. Experimental

Ingots of Mm $(Ni–Mn–Co–Al)_5$ (Mm = Ce-rich mischmetal, La: 28.26 wt.%; Ce: 50.47 wt.%; Pr: 5.41 wt.%; Nd: 15.86 wt.%; other rare earths: 0.3 wt.%) alloys were ground to a powder with a particle size of 20–63 μm. The alloy particles and 10 wt.% nickel powder were mixed with 2% polyvinyalcohol (PVA) into a paste, which was applied to a porous foamed substrate nickel dried in vacuum, and finally pressed at a pressure of 5000 kg cm^{-2}. The surface of the resulting electrode was treated by immersion in a 6 M KOH + 0.05 M KBH_4 solution at 70°C for 8 h.

A three-compartment glass cell separated with sintered glass was employed for electrochemical measurements. The MH electrode was placed in the central compartment and the two positive electrodes in compartments on each

* Corresponding author.

side. The positive electrodes had sufficiently larger electrochemical capacities than that of MH electrode. An Hg/HgO (6 M KOH) electrode was employed as a reference electrode; all electrode potentials are reported with respect to this electrode. The electrolyte was 6 M KOH + 20 g l^{-1} LiOH solution. Galvanostatic charge–discharge cycling tests were performed at room temperature (20–25°C). The MH electrode was charged for 3.5 h and discharged to −0.700 V after a rest period of 10 min, both at a constant current density of 100 mA g^{-1}.

High-rate dischargeability was determined from the ratio of discharge capacity at a given high, discharge current density to the discharge capacity at a current density of 100 mA g^{-1}. The exchange current density (J_0) was measured by linear sweep voltammetry (LSV) at a scan rate of 1 mV s^{-1} (Solartron 1286 electrochemical interface). In each run, the metal hydride electrode was designed to reach 50% depth of discharge. J_0 was calculated from the slope of the polarization curve in the vicinity of the rest potential using Eq. (1) [7]:

$$\frac{J}{V} = \frac{nFJ_0}{RT} \quad (1)$$

The apparent activation energy (E_a) of the MH electrode reaction was calculated from J_0 at different temperatures using Eq. (2) [8]

$$J_0 = A \exp \frac{-E_0}{RT} \quad (2)$$

where A is the constant in the range of experimental temperatures.

The composition and chemical state of the alloy surface were characterized with the aid of XPS (Perkin-Elmer PHI5300 ESCA System). The elements dissolved from the surface of alloys in a 6 M KOH solution were analyzed by ICP analysis. The specific surface-area of alloys was determined from gas (N_2) adsorption measurements, applying the BET method.

An AA-size Ni–MH battery was assembled with the KBH_4-treated MH electrode as the negative electrode. The discharge capacity of the Ni–MH battery was tested at the 0.2 C rate (discharge current at 1 C is 1000 mA) and 20°C. The high-rate dischargeability was evaluated from the ratios of the capacities at the 1 C, 3 C or 5 C rate to that at the 0.2 C rate. After charging for 4 h at 0.4 C at room temperature, the battery was held at −18°C. The low-temperature dischargeability was measured at the 0.2 C rate after 3 h.

3. Results and discussion

3.1. Activation property and discharge capacity

Typical discharge curves for the untreated and treated MH electrodes are shown in Figs. 1 and 2, respectively.

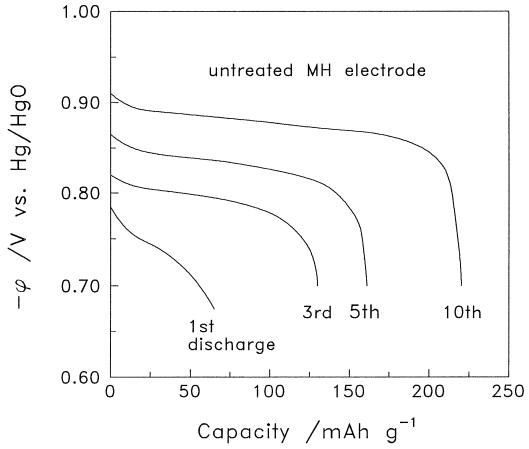

Fig. 1. Typical discharge curves of untreated MH electrode at 100 mA g^{-1}.

The discharge capacity of the untreated electrode is only 60 mA h g^{-1} on the first cycle, but increases steadily as the cycling continues. The capacity of the KBH_4-treated electrode exceeds 200 mA h g^{-1} even on the first cycle. The untreated MH electrode is completely activated only on the tenth cycle, whereas the KBH_4-treated electrode is completely activated on the third cycle. The variation in discharge capacity with cycling is shown in Fig. 3. The saturation capacities of the untreated and treated electrode are 220 and 270 mA h g^{-1}, respectively. After 400 cycles, the capacities of the untreated and treated electrodes decrease to 154 and 242 mA h g^{-1}, respectively, i.e., 70 and 91.2% of their corresponding saturation capacities. Thus, the reduction treatment of the MH electrode increases the discharge capacity and improves the activation property as well as the charge–discharge stability.

3.2. Hydrogen evolution reaction

The charging reaction of the hydride electrode consists of four processes: (i) charge transfer at the electrode/elec-

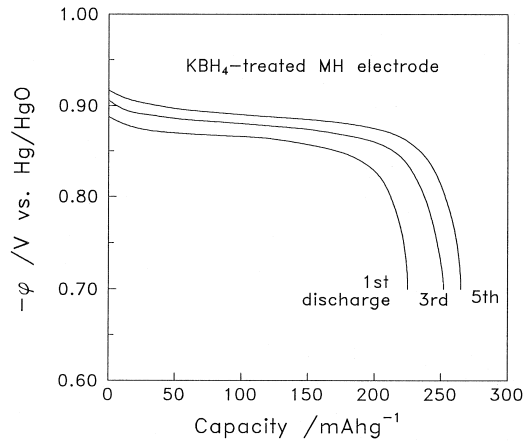

Fig. 2. Typical discharge curves of treated MH electrode at 100 mA g^{-1}.

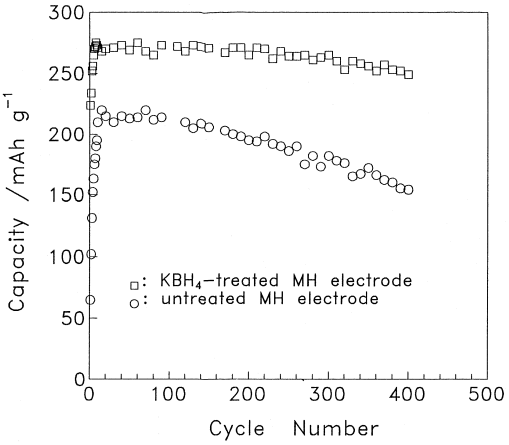

Fig. 3. Discharge capacity as a function of cycle number.

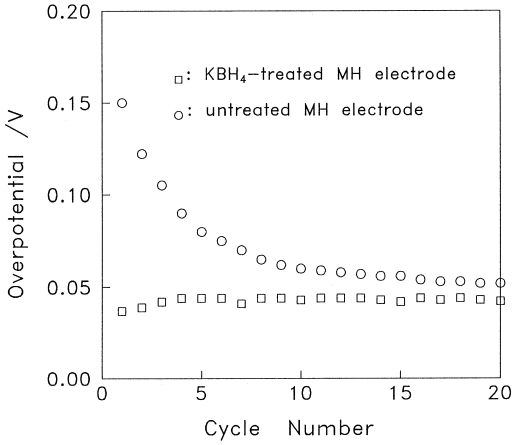

Fig. 5. Overpotential for hydrogen gas evolution of MH electrodes at charging current density of 100 mA g^{-1}.

trolyte interface; (ii) formation of hydrogen atoms on the surface of the alloy; (iii) diffusion of hydrogen into the bulk; (iv) evolution of hydrogen gas on combination of hydrogen atoms. The charging efficiency decreases as the hydrogen gas evolves. Hydrogen gas evolves much earlier on the untreated than for the treated MH electrode during charging, see Fig. 4. The volume of hydrogen gas collected on the untreated electrode is larger than that collected on the treated electrode for the same charge input. This means that the surface of the treated electrode has a higher affinity to hydrogen atoms and facilitates the diffusion of hydrogen into the bulk of the alloy to give an improved charging efficiency.

The evolution of hydrogen is the main electrode reaction in the latter stages of charging. The overpotential for this reaction is much lower for the treated electrode than for the untreated counterpart, especially during early charge–discharge cycles (see Fig. 5). For the untreated electrode, the overpotential amounts to approximately 150 mV on the first cycle and reduces to about 50 mV on cycle 20. For the KBH_4-treated electrode, however, the overpotential was only 40 mV even at the first cycle. This fact indicates that the surface reduction treatment improves electrocatalytic activity for hydrogen evolution.

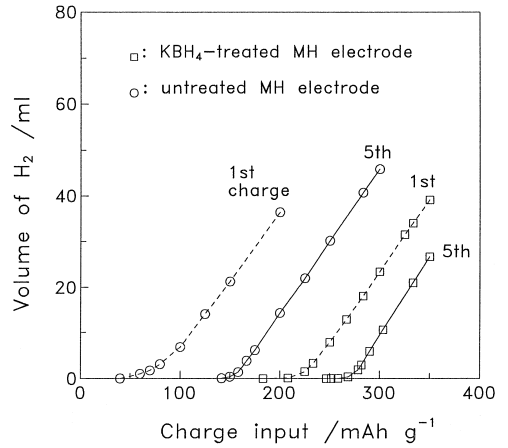

Fig. 4. Volume of hydrogen gas collected on MH electrodes as a function of charge input at a charge current density of 100 mA g^{-1}.

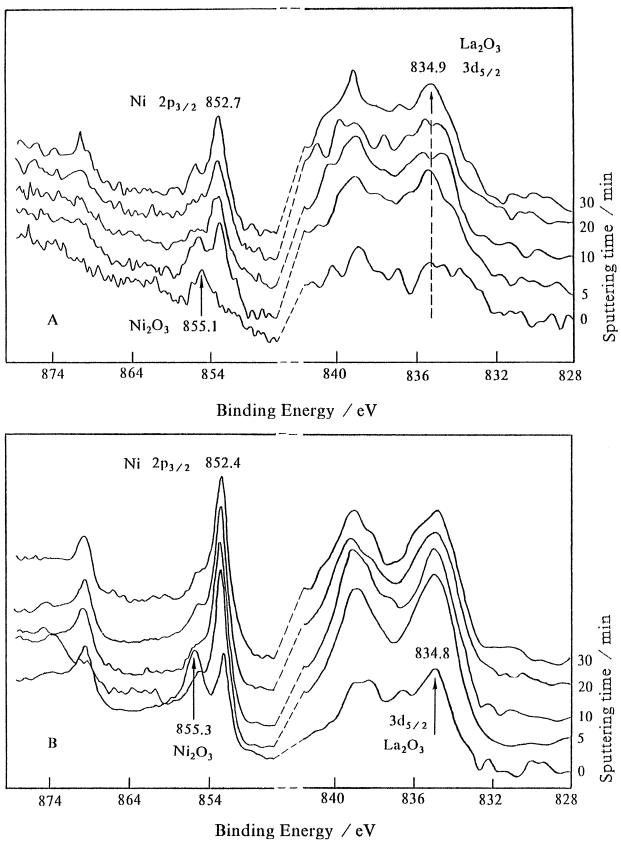

Fig. 6. The XPS spectra for surface of untreated (A) and treated (B) alloy.

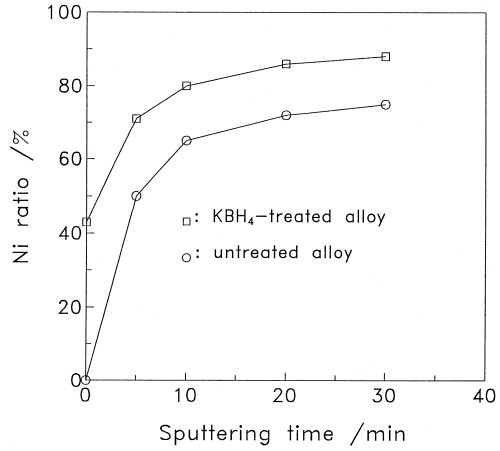

Fig. 7. Atomic ratio of Ni in the metallic to total Ni on surface of alloys.

3.3. Surface composition and chemical state of hydrogen-storage alloy

In general, the metal elements on the surface of hydrogen-storage alloys exist in the form of oxides. This is because they are oxidized easily. The oxide layer on the surface not only affects the activation and electrocatalytic activity but also interferes with the penetration of hydrogen into the crystal lattice during charging. The oxide film is generally removed by repeated charge–discharge cycling and, at the same time, the discharge capacity increases up to its saturation value after 10 to 15 cycles.

According to Iwakura et al. [9] and Matsuoka et al. [10], oxides on the surface of hydrogen-storage alloys could be reduced and even eliminated by the reduction treatment. However, according to the results of our XPS analysis, only nickel oxide is reduced, while the rare earth oxides are left intact after the reduction treatment. The spectra for the La $3d_{5/2}$ and Ni $2p_{3/2}$ levels of the treated and untreated alloys are shown in Fig. 6 as a function of sputtering time. The La on the surface of the both alloys is recognised to be La_2O_3. For the treated alloy, it is observed that part of Ni exists in the metallic state with its binding energy $E_b = 852.4$ eV. The ratio of Ni in the metallic state to total Ni is 49% on the surface and increases up to 72% after 5 min of argon sputtering (see Fig. 7). By contrast, no Ni in the metallic state exists on the surface of the untreated alloy.

Table 1
Amount of absorbed hydrogen and specific surface area of alloys vs. treatment time

Treatment time (h)	0	2	4	6	8
C_0 (mA h g^{-1})	0	15	41	84	150
A_s (m^2 g^{-1})	0.24	0.82	1.02	1.13	1.21

Table 2
Results of ICP analysis for elements dissolved into the solution during treatment (mol $l^{-1} \times 10^{-6}$)

La	Ce	Pr	Nd	Ni	Co	Mn	Al
0.567	8.21	6.65	7.01	no	no	13.0	432.1

Hydrogen is generally produced during the reduction reaction of the treatment. Some of this hydrogen is absorbed on to the electrode surface and then penetrates into the bulk to form hydride. The amount of absorbed hydrogen (C_0) can be determined by discharging at a definite current density (say 50 mA g^{-1}). The specific surface area (A_s) of the hydrogen-storage alloy increases after treatment. The results are listed in Table 1. The amounts of the elements dissolved from the alloy into solution during treatment, as determined by ICP analyses, are listed in Table 2. Aluminium and manganese are preferentially dissolved, but neither nickel nor cobalt can be found in the solution. The atomic relative ratio of La, Ce, Ni by XPS analysis is shown in Fig. 8. A Ni-rich surface layer with high electrocatalytic activity is thus produced because of the preferential dissolution, and this provides the MH electrode with high initial capacity, good activation, and low polarization.

3.4. High-rate dischargeability and exchange current density

The high-rate dischargeability of the treated and untreated MH electrodes was measured after complete activation. As shown in Fig. 9, the reduction treatment improved markedly the high-rate dischargeability. It is thought that the high-rate dischargeability is determined by the electrochemical kinetics on the surface and the diffusion rate of

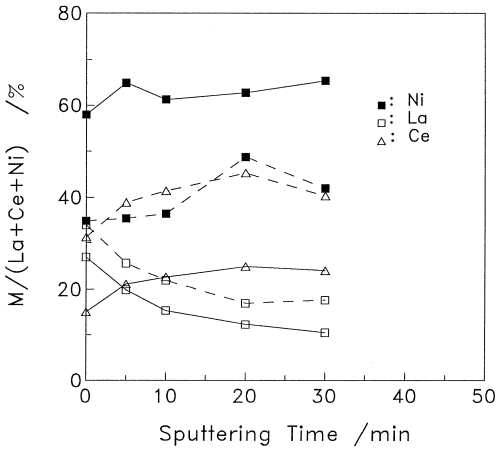

Fig. 8. Atomic relative ratio M/(La + Ce + Ni) (M = La, Ce, Ni) on surface of alloys.

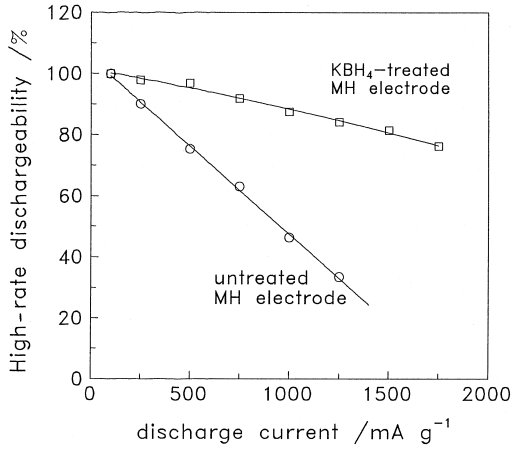

Fig. 9. High-rate dischargeability of treated and untreated MH electrodes.

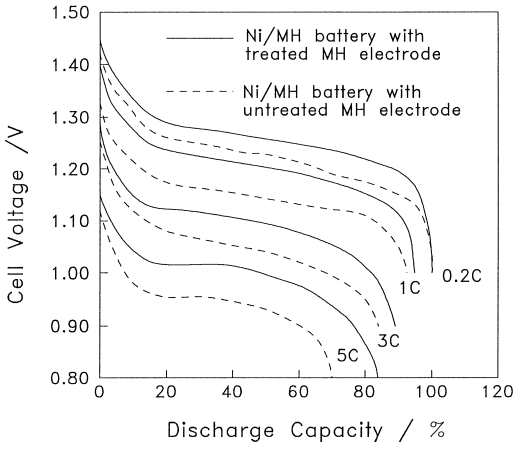

Fig. 11. Discharge curves of Ni-MH batteries at different rates.

hydrogen in the lattice. The surface of the treated alloy has high electrocatalytic activity and also often lower resistance to the diffusion of hydrogen. Therefore, both the electrochemical and the concentration polarization are decreased during charge and discharge at high-rates. The exchange current density of the untreated and treated MH electrode as a function of temperature is shown in Fig. 10. J_0 increases from 200 to 1200 mA g^{-1} when the electrode is treated. The apparent activation energies for the reaction of the treated and untreated electrodes are 21.3 and 33.7 kJ mol^{-1}, respectively, as deduced from Eq. (2). The electrochemical reaction on the surface of the alloy may be represented as follows:

$$M + H_2O + e \underset{\text{discharge}}{\overset{\text{charge}}{\Leftrightarrow}} M\text{–}H_{ad} + OH^- \quad (3)$$

By virtue of the Ni-rich layer produced on the surface and the increase in the specific surface area of the alloy, there is an enhancement of adsorption of the atomic hydrogen on the alloy surface and a decrease in E_a.

3.5. Ni–MH battery

The capacities of two AA-size Ni–MH batteries, one with a treated and the other with an untreated electrode as the negative, are both ~1150 mA h at 0.2 C, because the capacity of a battery is determined by the capacity of positive electrode ($Ni(OH)_2$/NiOOH). The plateau voltage during discharge is higher for the Ni–MH battery employing the treated electrode than for the battery with the untreated electrode. This means that the former battery has a higher power density. The high-rate dischargeability of the Ni–MH battery with treated electrode is also higher (see Fig. 11). Typical discharge curves at −18°C for the batteries are shown in Fig. 12. The capacity of the battery with the treated electrode at −18°C is more than 90% of

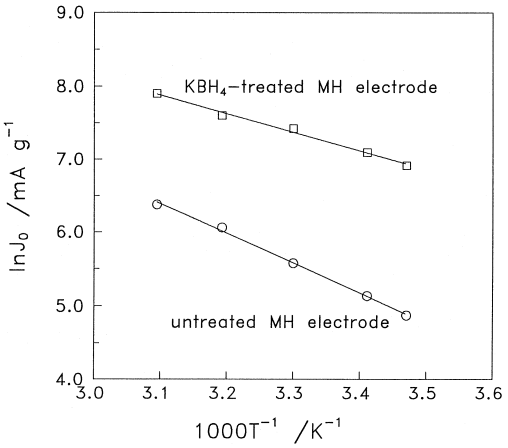

Fig. 10. Exchange current density of MH electrodes as function of temperature.

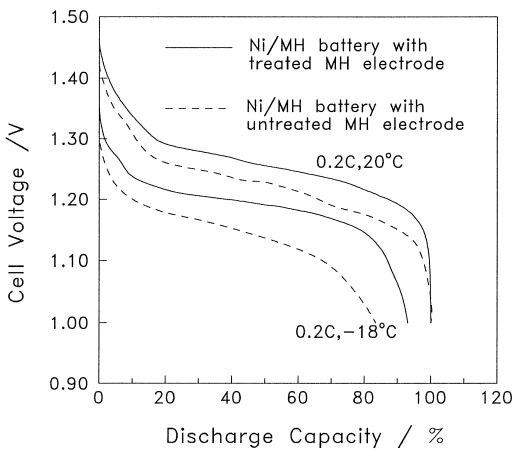

Fig. 12. Typical discharge curves for Ni-MH batteries at −18°C.

that at 20°C and 0.2 C. But the corresponding capacity of the battery with the untreated electrode is only 80% of that at 20°C and 0.2 C. This finding suggests that the simple reduction treatment also improves the high-rate dischargeability and low-temperature characteristics of the Ni–MH battery.

4. Conclusions

Many important performance parameters of the MH electrode, namely, the discharge capacity, activation, cyclic stability, electrocatalytic activity and high-rate dischargeability, are improved markedly by a reduction treatment. It is found that part of the nickel oxide on the surface of the alloys is reduced to metallic nickel which has electrocatalytic activity for electrochemical dissociation of water. Also, because of the preferential dissolution of aluminium and manganese, the specific surface area of the hydrogen-storage alloy increases. All these effects lead to an improvement in the performance of the MH electrode and, consequently, the Ni–MH battery.

Acknowledgements

This work is supported by the China National '863' program. We would like to thank Professor B.E. Conway for his help and guidance.

References

[1] J.J.G. Willems, Philips J. Res. 39 (1984) 1.
[2] C. Iwakura, M. Matsuoka, Prog. Batteries Battery Mater. 10 (1991) 81.
[3] C. Iwakura, T. Sakai, H. Ishikawa, Denki Kagaku 60 (1992) 680.
[4] M. Matauoka, M. Terashima, C. Iwakura, Electrochim. Acta 38 (1993) 1067.
[5] K. Natio, T. Matsuunami, K. Okuno, M. Mztsuoka, C. Iwakura, J. Appl. Electrochem. 24 (1994) 808.
[6] T. Sakai, H. Ishikawa, K. Oguro, C. Iwakura, H. Yoneyama, J. Electrochem. Soc. 134 (1987) 558.
[7] P.H.L. Notten, P. Hokkeling, J. Electrochem. Soc. 138 (1991) 1877.
[8] H. Yayama, A. Tomokiyo, K. Hirakawa, Jpn. J. Appl. Phys. 38 (1989) 530.
[9] C. Iwakura, M. Matsuoka, K. Asai, T. Kohno, J. Power Sources 38 (1992) 335.
[10] M. Matsuoka, K. Asai, Y. Fukumoto, C. Iwakura, Electrochim. Acta 38 (1993) 659.